Possible origin of the proton conduction mechanism of CsH_2PO_4 crystals at high temperatures

Jong-Ho Park*
Basic Science Research Institute, Pukyong National University, Busan 608-737, Korea
(Received 4 April 2003; revised manuscript received 11 August 2003; published 12 February 2004)

The high-temperature transformation of CsH_2PO_4 was studied by means of impedance spectroscopy, differential thermal analysis, and thermogravimetric methods. The dielectric constant showed a high-temperature anomaly around $T_p = 230\,°C$. The thermal transformation which appears around $T_p = 230\,°C$ is endothermic in addition to showing weight loss. Our results show evidence that the high-temperature transformation of CsH_2PO_4 near T_p is not a structural phase transition, but an onset of thermal decomposition of CsH_2PO_4 into $Cs_nH_2P_nO_{3n+1}$ [probably $n \gg 1$, $(CsPO_3)_n$] at reaction sites at the surface of the crystal. From complex ac impedance spectra, we observed impedance consisting of two regions for measuring frequency: the low-frequency region may be due to the formation and migration of H_2O molecules at the surface while the conduction mechanism of the high-frequency region seems to be Cole-Cole type and may be due to the proton migration in the bulk. Our results support that the phase of CsH_2PO_4 above T_p is not a superionic conductor phase caused by a structural transition (monoclinic→cubic) but rather a polymeric state caused by partial thermal decomposition. The possible origin of proton conduction for CsH_2PO_4 is considered to be the partial thermal decomposition of the crystal surface because the polymeric transition tends to increase breaking and reforming of the hydrogen bond at the surface.

DOI: 10.1103/PhysRevB.69.054104 PACS number(s): 77.84.Fa, 77.22.−d, 72.20.−i, 77.80.−e

I. INTRODUCTION

The low-temperature ferroelectric transition at T_c in KH_2PO_4 (KDP) and RbH_2PO_4 (RDP) crystals has been investigated for a long time by many researchers.[1–3] The high-temperature behavior of KDP and RDP crystals on heating above room temperature has also been studied.[4–25] A structural phase-transition-like phenomena, referred to as a high-temperature phase transition (HTPT), has been observed around T_p.[4–12] These crystals undergo successive phase transitions: at the upper transition point (T_p) from the monoclinic ($2_1 - C_2^2$ or $P2_1/m - C_{2h}^2$ for KDP and $2_1 - C_2^2$ or $P2_1/c - C_{2h}^2$ for RDP) high-temperature phase I to the tetragonal ($I\overline{4}2d - D_{2d}^{12}$ for KDP and RDP) intermediate-temperature paraelectric phase II, and at the lower transition point (T_c) to the orthorhombic ($Fdd2 - C_{2v}^{19}$ for KDP and RDP) low-temperature ferroelectric phase III. Based upon chemical analysis, many researchers have proposed that partial thermal decomposition sets in around T_p, corresponding to the following chemical reaction:[13–24]

$$nMH_2PO_4(s) \rightarrow M_nH_2P_nO_{3n+1}(s) + (n-1)H_2O(v) \quad (1)$$

$$(M = \mathrm{K, Rb, Cs, NH_4, Tl})$$

and claimed that the term HTPT should be replaced by the onset of partial polymerization at reaction sites on the surface of the crystal. Here, n is the number of molecules participating in thermal decomposition. The letter s or v enclosed in parentheses denotes that the corresponding compound is in the solid or vapor state, respectively.

Recently, Park *et al.* confirmed that phase I of KDP and RDP is not the monoclinic phase, but related to a chemical change [KH_2PO_4 (phase II)→$K_2H_2P_2O_7$ (phase I) and RbH_2PO_4 (phase II)→mixture consisting mainly of RbH_2PO_4 and $Rb_2H_2P_2O_7$ (phase I)] such as thermal decomposition; their report was based on dielectric constant, thermal analysis, and thermomicroscopy data.[16–20] Using x-ray and thermal analysis Oritz *et al.*[22–24] supported the idea that the high-temperature phenomena in KH_2PO_4 and RbH_2PO_4 are effects of thermal decomposition.

CsH_2PO_4 (CDP) is a member of the KDP family of H-bonded crystals.[1] This crystal has a transition sequence similar to that in KDP and RDP though the crystal structures are different. The CDP crystal undergoes the following three phase transitions:[25–33]

$$\begin{array}{ccccc} \textbf{Ferroelectric} & & \textbf{Paraelectric} & & \textbf{Superionic} \\ \textbf{Phase III} & \xrightarrow{T_c = -120\,°\mathrm{C}} & \textbf{Phase II} & \xrightarrow{T_p = -230\,°\mathrm{C}} & \textbf{Phase I} \\ \text{Monoclinic} & & \text{monoclinic} & & \text{Cubic ?} \\ (P2_1 - C_2^2) & & (P2_1/m - C_{2h}^2) & & (mmm - D_{2h}) \end{array}$$

Rapoport reported the transition temperatures on heating with fast heating rates of 42–90 °C/min by differential thermal analysis (DTA) and differential scanning calorimetry (DSC) as follows:[27] $T_c = -120\,°C$, $T_c' = 149\,°C$, $T_p = 230\,°C$, and 345 °C for CDP. In their x-ray study, Bronowska *et al.* reported that the lattice parameter changes deviate considerably from linearity on heating above 149 °C, but the space group of the crystal above 149 up to 230 °C does not change ($P2_1/m-C_{2h}^2$).[30] Rashkovich *et al.* found transitions at 230 °C (T_p) and 265 °C (T_p').[28] Wada *et al.* showed that the transition at $T_p=230$ °C was confirmed, but the one at $T_c'=149$ °C was not.[29] Baranov *et al.* reported a sudden ionic conductivity jump around $T_p=230$ °C through the measurement of the temperature dependence of the bulk conductivity in a CDP single crystal. They studied the properties of the HTPT and electrical conductivity, and claimed that the high-temperature cubic phase above 230 °C in CDP was a superionic conduction phase. From their study of fast *D-H* isotopic exchange, it was also suggested that CDP is a superprotonic conductor.[25,26] Bronowska recently performed powder x-ray measurements of CDP in an H_2O-saturated atmosphere and observed a phase transition at about 231 °C from monoclinic CDP to cubic CDP without decomposition.[31] Otomo *et al.* proposed that a steep change in the conductivity of pressed powder of poly-H-bonded crystals CDP due to a phase transition from a low conductive phase to a high conductive phase (superionic conduction phase) occurs reversibly at around 230 °C under humid conditions.[32] Using Brillouin spectroscopy Luspin *et al.* reported that on heating a CDP crystal above room temperature, it undergoes two polymeric transitions:[33] the first one near 120 °C (weakly marked) and a second one at 230 °C (the well marked superionic transition). These discrepancies of the different research groups seem to be caused by the difference in experimental humidity conditions. Thus, the transition point at $T_c'=149$ °C is still uncertain, and it is also possible that the HTPT of CDP around $T_p=230$ °C is not related to a structural phase transition but to thermal decomposition such as in KDP, RDP, and KH_2AsO_4 (KDA) crystals.[16–24]

However, hydrogen bonds (H bonds) play a dominant role in determining the properties of crystals such as acid phosphates and arsenates, and many studies have been made on the nature of the H bonds in these materials.[34] It is generally found that the H bonds which are part of a three-dimensional network show enhanced effects in dielectric, ferroelectric, thermal, and other properties when compared with similar effects in crystals containing isolated H bonds. The transport properties of protons in such crystals may be treated in terms of proton defects, using the same basic models that have been extensively used in studies on alkali halides and other ionic crystals. Several conduction studies have been made on H-bonded crystals of the type related to the structural phase transition at high temperature studied in Refs. 25, 26, 35–39 But Park *et al.* suggested that mechanisms of the electrical conductivity in H-bonded crystals must consider thermal decomposition as well as ionic transport because it is known that many H-bonded crystals reveal surface instabilities such as thermal decomposition at high temperature.[16,18,21,22] Therefore, we studied the high-temperature phenomena and electrical conduction mechanisms of CDP by means of thermal analysis and impedance spectroscopy.

II. EXPERIMENTAL

Crystals of CDP were synthesized by the reaction $CsOH + H_3PO_4 \rightarrow CsH_2PO_4 + H_2O$ with pH=4. The resultant solution was heated to about 80 °C in order to remove H_2O and induce incipient crystallization. The obtained polycrystals were dried and recrystallized. The acidity of the solutions were controlled in order to obtain good morphology of the CDP monoclinic crystals. Single crystals were grown by evaporation at 35 °C from the aqueous solution. Samples were cut from the clear tips of the crystal, the one perpendicular to the *b* axis, and were polished first with No. 1000 sand paper and then with velvet cloth. The electrodes were prepared with conducting silver paint. The complex ac impedance (Z^*) was determined in the frequency range from 1 to 3×10^6 Hz using an impedance analyzer (SI1260). Samples were kept in an electric furnace whose temperature was controlled with a Pt-Pt(Rh) thermocouple. The rate of the temperature variation was 0.2 °C/min. Crystal fragments were used in DSC and thermogravimetric (TGA) experiments. The DSC and TGA studies were performed in the temperature range from 30 to 550 °C using a differential scanning calorimeter (Perkin-Elmer, U.S.A., TGA7) and thermogravimeter (Perkin-Elmer, U.S.A., Pyrisl). The rate of the temperature variation was 5 °C/min.

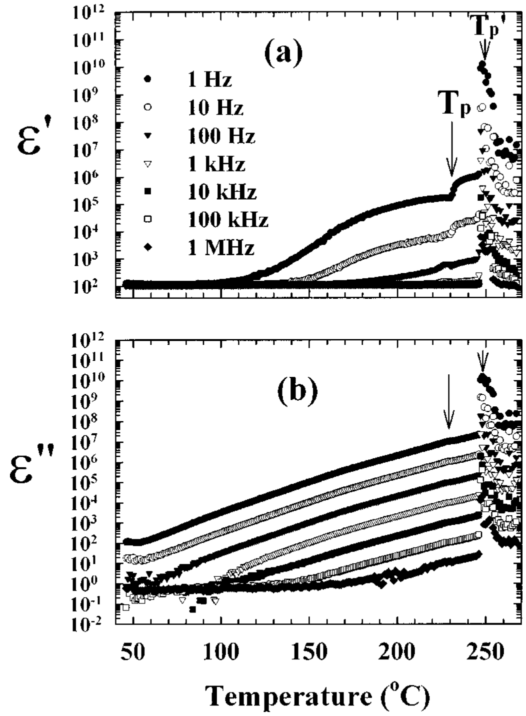

FIG. 1. Temperature dependence of (a) ε_b' and (b) ε_b'' of the complex dielectric constant of CsH_2PO_4 at various frequencies. The heating rate is 0.2 °C/min.

III. RESULTS AND DISCUSSION

Figures 1(a) and 1(b) show the real (ε_b') and imaginary (ε_b'') parts of the complex dielectric constant along the *b* axis, in the temperature range between 30 and 270 °C at several frequencies with measuring temperature interval 1.0 ± 0.2 °C. Dispersion of ε_b' begins at temperature 100 °C. On raising the temperature, ε_b' suddenly increases to nearly its high-temperature value at about $T_p=230$ °C. It has a discon-

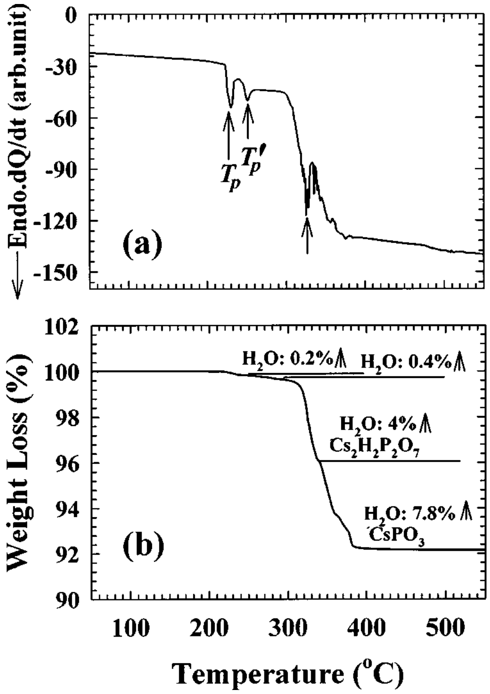

FIG. 2. (a) DSC and (b) TGA curves for CsH_2PO_4 heated in air to 550 °C at a heating rate of 5 °C/min.

tinous large increase near $T_p' = 250$ °C after further heating. It decreases again during further heating. The values of ε_b'' are shown to depend almost inversely on the measuring frequencies. This agrees with the well known fact that ε_b'' is related to the ionic conductivity σ as $\varepsilon_0 \omega \varepsilon_b''$,[40] where ω is the frequency of the applied field and ε_0 the vacuum permittivity. ε_b'' increases gradually because the electrical conductivity increases on heating above room temperature. The extremely high values of ε_b' at low frequency and high temperature evidence phase-shifted conductivity.

If the high-temperature phase transition of CDP at T_p is caused by thermal decomposition, decrease of weight and thermal change may appear in thermal analysis. The DSC and TGA experiments were performed with heating rates of 5 °C/min in an open atmosphere. As shown in Figs. 2(a) and 2(b), the thermal transformation shows an endothermic peak at $T_p = 230$ °C; the onset of weight loss at $T_p = 225$ °C for CDP indicates the beginning of thermal decomposition. These temperatures may correspond to the so-called high-temperature transition temperature. On heating further, beyond T_p, the thermal transformations which occur at $T_p' = 250$ and 325 °C in CDP give rise to several endothermic peaks. Atmospheric pressure DSC studies of CDP on heating above room temperature revealed two transitions: a quasi-irreversible transition at 149 °C (T_c') and a second reversible transition at 230 °C (T_p).[27] Wada *et al.* showed that the transition at 230 °C was confirmed but the one at 149 °C was not.[29] We also could not detect a transition at 150 °C on heating. The present result seems to agree with that of Wada *et al.* and disagree with those of Refs. 27, 30.

The transformation temperatures corresponding to the DSC signals indicating weight losses are commonly believed to indicate high-temperature phenomena caused by thermal decomposition processes such as Eq. (1). For comparisons with TGA results and theory, the possible products are calculated and based on Eq. (1). The ratio of the changed products (polymerization) and escaped products (H_2O) are related to chemical changes in the CDP for the various possible n values as follows.

The case of $n=2$, $2CsH_2PO_4 \rightarrow Cs_2H_2P_2O_7 + H_2O$. Ratio of changed product:

$$\frac{M(Cs_2H_2P_2O_7)}{M(2CsH_2PO_4)} \times 100 = 96.08\%.$$

Ratio of escaped product:

$$\frac{M(H_2O)}{M(2CsH_2PO_4)} \times 100 = 3.92\%.$$

The case $n \gg 1$, $nCsH_2PO_4 \rightarrow Cs_nH_2P_nO_{3n+1} + (n-1)H_2O$. Ratio of changed product:

$$\frac{M(Cs_nH_2P_nO_n)}{M(nCsH_2PO_4)} \times 100 \approx \frac{M(CsPO_3)}{M(nCsH_2PO_4)} \times 100 = \frac{M(CsPO_3)}{M(CsH_2PO_4)} \times 100 = 92.16\%.$$

Ratio of escaped product:

$$\frac{M[(n-1)H_2O]}{M(nCsH_2PO_4)} \times 100 \approx \frac{M(nH_2O)}{M(nCsH_2PO_4)} \times 100 = \frac{M(H_2O)}{M(CsH_2PO_4)} \times 100 = 7.84\%,$$

where M is the atomic weight. One finds a semiplateau region, accompanied by about 0.2% weight loss between 235 and 245 °C. Weight loss begins around 250 °C, and the other semiplateau region was found between 260 and 290 °C at about 0.4% weight loss. For any given n value, the weight losses at the semiplateau are not the same as the values calculated for the intermediate products. The range of existence of $Cs_2H_2P_2O_7$ in the case of $n=2$ corresponds to 340–350 °C because for the intermediate products the calculated and measured weight loss are the same. As shown in Figs. 2(a) and 2(b), this weight loss is indicative of the formation of various polymers, during the course of dehydration to the final formation of $CsPO_3$. The final product corresponds to a change from CsH_2PO_4 to $CsPO_3$ (weight loss 7.8%) above 380 °C, because the calculated value and measured weight loss are the same. But the temperature regions (230–245 °C and 260–290 °C), over which the weight changes, are difficult to explain, since the processes of polymerization depend on temperature and the intermediate product is unstable. If we adopt the realistic phase relationships of Eq. (1), the HTP slightly above T_p is not a single phase of CsH_2PO_4, but a mixture consisting mainly of CsH_2PO_4 and $Cs_2H_2P_2O_7$. The temperature regions of weight loss in CDP could be related to mixed phases. Generally, thermal decomposition phenomena tend to occur at surfaces where heat contact is direct and

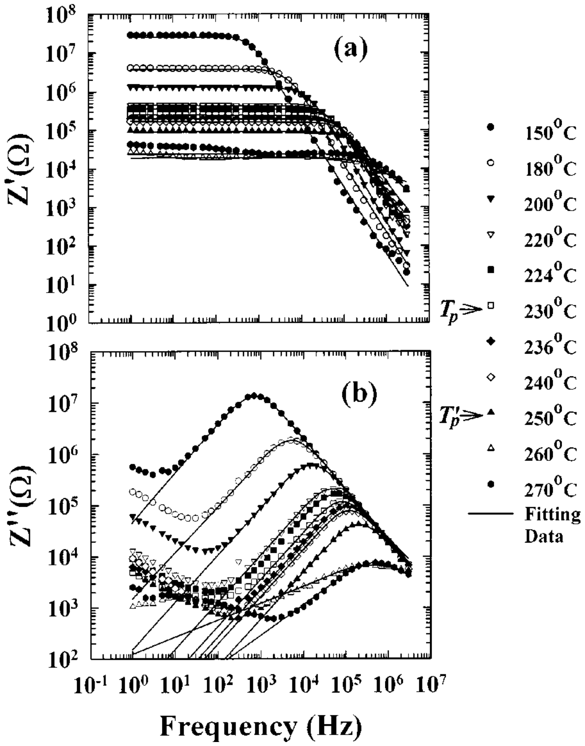

FIG. 3. Impedance spectra of (a) Z_b' and (b) Z_b'' in CsH_2PO_4. The solid line represents a fit to Eq. (2).

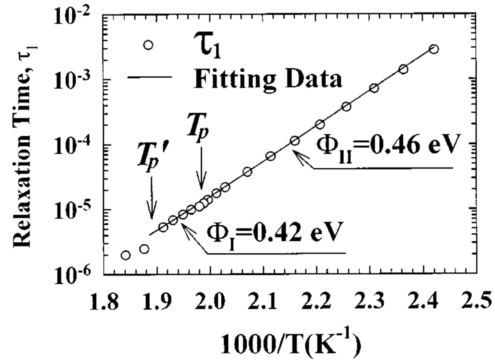

FIG. 4. Temperature dependence of relaxation time in seconds τ_1 on $1/T$ in CsH_2PO_4. Solid lines fitted by Eq. (3). The slope of the straight lines corresponds to the activation energy.

chemical binding is weaker, rather than in the bulk of a crystal. Therefore, the results of our TGA indicated that the high-temperature phenomena exhibited by CDP near T_p should be interpreted as indicating the *onset of partial polymerization at reaction sites on the surface,* such as represented by Eq. (1).

One must consider the dc bulk effect to understand electrical conduction in CDP because our TGA curve indicates that the high-temperature transformation is caused by partial thermal decomposition at the surface rather than a structural phase transition. Figures 3(a) and 3(b) present the variation of the real (Z_b') and the imaginary (Z_b'') parts of the impedance versus frequency using a double logarithmic scale for several temperatures. It is observed that, above and below T_p, Z_b' decreases slowly up to a frequency of 10^3 to 10^6 Hz, depending on the temperature and then continuously decreases with increasing frequency approximately as $1/\omega$. The relaxational peak frequency of Z_b'' moves to higher frequency with increasing temperature. The absolute values of the high-frequency slopes are, in fact, very close to unity and seem to be independent of the temperature. In the low-frequency region, dispersion of Z_b'' begins above 100 °C and increases with increasing of temperature, and another relaxational peak frequency of Z_b'' appeared above T_p. That is, the low-frequency slopes have values lower than unity and are strongly temperature dependent. These two different tendencies in the temperature dependence suggest that two dispersion mechanisms are involved. Considering the existence of the dispersion mechanism in the high-frequency region and the bulk conductance (G_1) of the material, an alternative model may be proposed and written as the Cole-Cole expressions[40]

$$Z^*(\omega) = \frac{1/G_1}{1+(i\omega\tau_1)^m},$$

$$\tau_1 = 1/\omega_{p1}, \tag{2}$$

where ω_{p1} is the characteristic angular frequencies determined from relaxation times τ_1. The solid lines in Fig. 3(b) are theoretical curves obtained by using Eq. (2). Only the data relative to the imaginary part were used in the fitting. The three parameters m, τ_1, and G_1 were then introduced into the real part of the formula to check whether the calculated values are also in agreement with the measured value of Z_b'. The agreement between experimental and calculated values for both real and imaginary parts of the impedance confirms that the model proposed here is pertinent to the description of the high-temperature behavior of CDP. The parameters m take values over the entire range $0 \leqslant m \leqslant 1$ and may be functions of temperature. The fitting of Eq. (2) for the b-axis case always leads to a value of m close to about unity.

The loss peak frequency ω_{p1} is obtained by fitting the imaginary impedance data to Eq. (2) and the variation of relaxation times $\tau_1 = 1/\omega_{p1}$ as a function of reciprocal temperature is shown in Fig. 4. τ_1 can be described by an Arrhenius behavior as given by

$$\tau_1 = \tau_0 \exp(\Phi/k_B T) \tag{3}$$

with the natural relaxation time τ_0 and activation energy Φ. τ_1 has a knee around $T_p = 230$ °C and a small jump around $T_p' = 250$ °C. The activation energies estimated are $\Phi_{II} = 0.46$ eV below T_p and $\Phi_I = 0.42$ eV above T_p for τ_1.

The dc bulk conductivity can be analyzed by means of complex impedance formalism. Two methods can be used to obtain the dc bulk conductance ($G_1 = G_{dc,B}$). The first method consists of extrapolating the circular arc to the real axis at the low-frequency end of Z'' vs Z', the complex impedance plot. As seen in Figs. 3(a) and 3(b), the complex impedance obtained from experimental data satisfy Eq. (2) well (solid line). So, a second method based on fitting by Eq. (2) has been used to determine G_1.[40] Figure 5 shows G_1 of CDP along the b axis. G_1 has a knee around $T_p = 230$ °C and a small jump around $T_p' = 250$ °C. We can see a good linear-

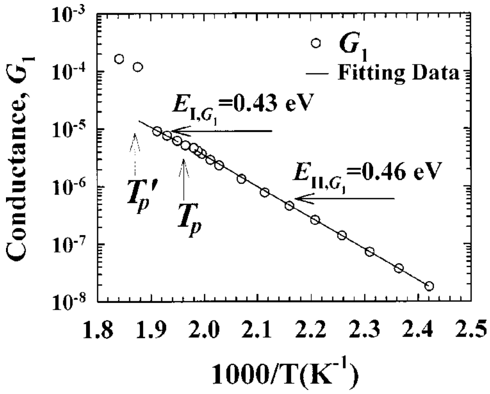

FIG. 5. Temperature dependence of G_1 of CsH_2PO_4 crystals. Solid lines are fitted by Eq. (4). The slope of the straight lines corresponds to the activation energy.

ity between $\ln(G_1)$ and $1/T$ as shown in Fig. 5. These results can be described by the Arrhenius behavior

$$G_1 \sim \exp(-E/k_B T). \tag{4}$$

with the dc bulk activation energy E and Boltzmann constant k_B. The dc bulk electrical conductance (open circles) obtained from experimental impedance data satisfy the Arrhenius relation well (solid line). The value of activation energies $E_{\mathrm{II},G1} = 0.46$ eV below T_p and $E_{\mathrm{I},G1} = 0.43$ eV above T_p in CDP, are obtained from the slopes of theoretical fitting of an Arrhenius relation such as Eq. (4). There are considerable differences in the published reports and our work concerning the activation energy, but the values of E_{G1} are similar to our results as shown in Fig. 4. Baranov *et al.* reported that the activation energies are about 0.3 eV above T_p and 0.99 eV below T_p, and that the conduction occurs through proton migration. They claimed that the high-temperature phase above 230 °C in CDP is a superionic conduction phase.[26] Generally, the main difference between superionic and ionic conductors concerns the activation energy of the ionic conductivity.[34] For the former, which are also called fast ionic conductors, E_a is lower than 0.40 eV and σ is higher than $\sim 10^{-3}\ \Omega^{-1}\,\mathrm{cm}^{-1}$ while values varying between 0.6 and 1 eV are usually observed for normal ionic conductors, with conductivities lower than $\sim 10^{-3}\ \Omega^{-1}\,\mathrm{cm}^{-1}$. The state of our CDP crystal in the temperature region from 230 to 250 °C is not superionic according to this definition, because our $E_a = 0.43$ eV is higher than 0.40 eV.

At temperature ranges of room temperature or below and T_p or below, the dielectric and conductive behavior of the KDP family is known as follows: Schmidt suggested that proton intrabond transfer in O—H···O bonds is the mechanism for dynamic behavior of rubidium/ammonium dihydrogen phosphate mixed crystals.[2] Because of the strong proton-proton interaction, such transfer is associated with thermally activated creation of H_3PO_4 and HPO_4 intrinsic "Takagi" defects, their hindered diffusion in a random-step fractal potential, and their eventual annihilation. This "bond charge semiconductivity" mechanism does not contribute to dc conduction. The orientational defects D (two hydrogens within the O···O bond) or L (lack of hydrogen), are proposed.[34]

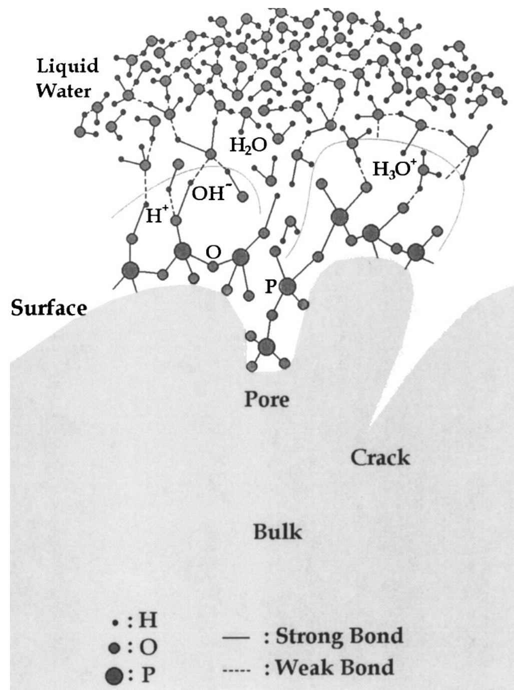

FIG. 6. Schematic illustration of the process of thermal decomposition at the surface for a CDP crystal. Microscopic (atomistic) view of the high-temperature phenomena $MH_2PO_4(s) \rightarrow M_nH_2P_nO_{3n+1}(s) + (n-1)H_2O(g)$ by which water layers can be formed at the surface.

They thermally formed in pairs by interbond jumping between different O—H···O bonds, but migrate individually. Sharon and Kalia[38,39] have studied the dc electrical conduction of KDP and KDA single crystals and have proposed a mechanism of synchronous rotation of the H_2PO_4 group. They have concluded that the enthalpy for the experimental results is related to the enthalpy for the rotation of the phosphate group rather than to the enthalpy for the formation of the defects (L, D). Proton dc conduction is thus expected to be related to the presence of D or L defects.

Most investigators studying electrical conductivity seem to pass over the decomposition effect. However, from our TGA results there is around 4% of weight loss near T_p, and we calculate a result for which the curve of weight loss [Fig. 2(b)] is based on Eq. (1). Therefore, we consider the electrical conductivity mechanism above T_p for the CDP crystal that includes the partial break up of hydrogen bonds and the formation of H_2O molecules by thermal decomposition at the crystal surface, as illustrated in Fig. 6. Associated processes as formation of chains of P—O—P bonds, and liberation of H_2O molecules from the surface. Two mechanisms of impedance relaxation in CDP at high temperature can involve crystal defects induced by water molecules caused by thermal decomposition and dehydration at the surface is reflected in the low frequency relaxation of the impedance. To summarize, the mechanism of the electrical conductivity may be partial break up of hydrogen bonds and the formation of H_2O molecules at or near the crystal surface as well as proton migration in the bulk.

IV. CONCLUSIONS

In summary, the high-temperature transformation of CDP was studied by means of impedance spectroscopy, differential thermal analysis, and thermogravimetric methods. The dielectric constant showed a high-temperature anomaly around $T_p = 230\,°\mathrm{C}$. The thermal transformation which appears around $T_p = 230\,°\mathrm{C}$ is endothermic in addition to showing weight loss. We separated bulk conductivity by means of a complex impedance formalism. The bulk activation energies are obtained $E = 0.46\,\mathrm{eV}$ below T_p and $E = 0.43\,\mathrm{eV}$ above T_p. Our results show evidence that the high-temperature transformation of CDP near T_p is not a structural phase transition, but an onset of thermal decomposition of CsH_2PO_4 into $Cs_nH_2P_nO_{3n+1}$ [probably $n \gg 1$, $(CsPO_3)_n$]. The possible origin of high-temperature anomalies in the proton conduction in CDP is considered to be the partial thermal decomposition of the crystal surface because a polymeric transition tends to increase breaking and reforming of the hydrogen bond at the surface.

ACKNOWLEDGMENTS

This work was supported by the Korea Research Foundation (Grant No. KRF-2002-070-C00042).

*Electronic address: parkkdp@hanafos.com

[1] For example, see Ferroelectrics **71** (1987); **72** (1987) (special issue on KH_2PO_4-type ferroelectrics and antiferroelectrics).

[2] V. H. Schmidt, J. Mol. Struct. **177**, 257 (1988); Ferroelectrics **78**, 207 (1988).

[3] V. H. Schmidt, S. Lanceros-Mendez, S. C. Meschia, and N. J. Pinto, Solid State Ionics **125**, 147 (1999).

[4] R. Blinc, V. Dimic, D. Kolar, G. Lahajnar, J. Stepisnik, S. Zumer, N. Vene, and D. Hadzi, J. Chem. Phys. **49**, 4996 (1968).

[5] J. Grunberg, S. Levin, I. Pelah, and D. Gerlich, Phys. Status Solidi B **49**, 857 (1972).

[6] B. M. Zhigarnovskii, Yu A. Polyakov, V. I. Bugakov, M. A. Maifat, K. Rakhimov, N. G. Moisashvili, O. G. Takaishvili, A. G. Mdinaradze, and V. P. Orlovskii, Inorg. Mater. (Transl. of Neorg. Mater.) **20**, 1074 (1984).

[7] E. Rapoport, J. B. Clark, and P. W. J. Richter, Solid State Chem. **24**, 423 (1978).

[8] B. Baranowski, M. Friesel, and A. Lunden, Z. Naturforsch. A **42**, 565 (1987).

[9] Y. Shapira, S. Levin, D. Gerlich, and S. Szapiro, Ferroelectrics **17**, 459 (1978).

[10] J. Seliger, V. Zagar, and R. Blinc, Phys. Rev. B **47**, 14 753 (1993).

[11] B.-K. Choi and S. C. Chung, Ferroelectrics **155**, 153 (1994).

[12] M. O'Keeffe and C. T. Perino, J. Phys. Chem. Solids **28**, 1086 (1966).

[13] K.-S. Lee, J. Phys. Chem. Solids **57**, 333 (1996).

[14] J. A. Subramony, B. J. Marquardt, J. W. Macklin, and B. Kahr, Chem. Mater. **11**, 1312 (1999).

[15] J. A. Subramony, S. Lovell, and B. Kahr, Chem. Mater. **10**, 2053 (1998).

[16] J.-H. Park, K.-S. Lee, J.-B. Kim, and J.-N. Kim, J. Phys.: Condens. Matter **8**, 5491 (1996); **9**, 9457 (1997).

[17] J.-H. Park, K.-S. Lee, and J.-N. Kim, J. Korean Phys. Soc. **32**, S1149 (1998).

[18] J.-H. Park, K.-S. Lee, and J.-N. Kim, J. Phys.: Condens. Matter **10**, 9593 (1998).

[19] J.-H. Park, Solid State Commun. **123**, 291 (2002).

[20] J.-H. Park, K.-S. Lee, and B.-C. Choi, J. Phys.: Condens. Matter **13**, 9411 (2001).

[21] J.-H. Park, J. Phys. Soc. Jpn. **71**, 2715 (2002).

[22] E. Ortiz, R. A. Vargas, and B.-E. Mellander, J. Phys. Chem. Solids **59**, 305 (1998).

[23] E. Ortiz, R. A. Vargas, B.-E. Mellander, and A. Lunden, J. Chem. Phys. **71**, 1797 (1997).

[24] E. Ortiz, R. A. Vargas, G. Cuervo, B.-E. Mellander, and J. Gustafson, J. Phys. Chem. Solids **59**, 1111 (1998).

[25] A. I. Baranov, V. P. Khiznichenko, and L. A. Shuvalov, Ferroelectrics **100**, 135 (1989).

[26] A. I. Baranov, V. P. Khiznichenko, V. A. Sandler, and L. A. Shuvalov, Ferroelectrics **81**, 183 (1988).

[27] E. Rapoport, J. B. Clark, and P. W. Richter, J. Solid State Chem. **24**, 423 (1978).

[28] L. N. Rashkovich and K. B. Meteva, Kristallografiya **23**, 796 (1978) [Sov. Phys. Crystallogr. **23**, 447 (1978)].

[29] M. Wada, A. Sawada, and Y. Ishibashi, J. Phys. Soc. Jpn. **47**, 1571 (1979).

[30] W. Bronowska and A. Pietraszko, Solid State Commun. **76**, 293 (1990).

[31] W. Bronowska, J. Chem. Phys. **114**, 611 (2001).

[32] J. Otomo, N. Minagawa, C.-J. Wen, K. Eguchi, and H. Takahashi, Solid State Ionics **8814**, 1 (2002).

[33] Y. Luspin and P. Simon, Solid State Commun. **118**, 189 (2001).

[34] Ph. Colomban and A. Novak, *Proton Conductors*, edited by Ph. Colomban (Cambridge, Cambridge University Press, 1992), pp. 165–182.

[35] D. Abramic, J. Dolinŝek, R. Blinc, and L. A. Shuvalov, Phys. Rev. B **42**, 442 (1989).

[36] F. Qi, M. Winterich, A. Titze, and R. Böhmer, J. Chem. Phys. **117**, 10233 (2002).

[37] L. B. Harris and G. J. Vella, J. Chem. Phys. **58**, 4550 (1973).

[38] M. Sharon, J. Solid State Chem. **27**, 263 (1979).

[39] M. Sharon and Anjan K. Kallia, J. Solid State Chem. **21**, 171 (1977).

[40] A. K. Jonscher, *Dielectric Relaxation in Solids* (Chelsea Dielectrics Press, London, 1983).